Science in China Series G: Physics, Mechanics & Astronomy

www.scichina.com
phys.scichina.com
www.springerlink.com

Large eddy simulation of compressible turbulent channel flow with spanwise wall oscillation

FANG Jian[1†], LU LiPeng[1] & SHAO Liang[2]

[1] National Key Laboratory on Aero-engines, School of Jet Propulsion, Beihang University, Beijing 100191, China;
[2] Laboratory of Fluid Mechanics and Acoustics, Ecole Centrale de Lyon, France

The influences of the modification of turbulent coherent structures on temperature field and heat transfer in turbulent channel flow are studied using large eddy simulation (LES) of compressible turbulent channel flows with spanwise wall oscillation (SWO). The reliability of the LES on such problems is proved by the comparisons of the drag reduction data with those of other researches. The high consistency of coherent velocity structures and temperature structures is found based on the analyses of the turbulent flow field. When the coherent velocity structures are suppressed, the transportations of momentum and heat are reduced simultaneously, demonstrating the same trend. This shows that the turbulent coherent structures have the same effects on the transportations of momentum and heat. The averaged wall heat flux can be reduced with appropriate oscillating parameters.

large eddy simulation, spanwise wall oscillation, compressible, temperature field, heat transportation

The spanwise wall oscillation (SWO) is an effective drag reducing technique to suppress turbulence activity. It was first studied in 1992 by Jung et al.[1,2], who got the continual reductions of drag (40% the maximum), turbulence intensity and density of coherent structures. After the work of Jung[1,2], Laadhari et al.[3] carried out the experimental research on the problem in the water channel, and validated the conclusions of Jung[1,2]. After that, lots of researchers carried out the numerical (Baron et al.[4], Orlandi et al.[5], Dhanak et al.[6], Quadrio et al.[7], Choi et al.[8], Huang et al.[9,10], Quadrio et al.[11], Zhou et al.[12], Riccoa et al.[13]) and experimental (Trujillo et al.[14], Choi et al.[15−18], Cicca et al.[19], Iuso et al.[20], Ricco et al.[21]) researches on this problem, and they came to the consistent results with those of Jung et al.[1,2]. Among them, Orlandi et al.[5], Quadrio et al.[7] and Choi et al.[16] carried out the numerical and experimental researches on the pipe flow oscillating around its axis. The maximum drag reduction of 25% and some similar results as in channel flows were reached.

The SWO has drawn so much attention in recent decades, due to the dramatic drag reduction as a large scale control technique (the maximum drag reduction of 45% can be reached according to Choi et al.[15], contrastively, the riblets can only reach the level of 10%) and the connections with the dynamic mechanisms of self-sustaining process and regeneration of turbulence. Choi et al.[15] figured that, the reduction of drag was mainly caused by the negative spanwise vorticity in the near wall region which was generated by the interaction between streamwise vortex and induced Stokes layer by SWO. They also observed the distortion of streaks in the flow with oscillating wall. However, Baron et al.[4] and Dhanak et al.[6] figured out that the mechanism of the drag reduction was the movement of low-speed streaks related to the longitudinal vortices, which disturbed the spatial coherence between the longitudinal vortices and the low-speed streaks, and caused the weakening of the streaks. Based on the turbulence regeneration mecha-

Received September 9, 2008; accepted November 10, 2008
doi: 10.1007/s11433-009-0165-3
†Corresponding author (email: fangjian@sjp.buaa.edu.cn)
Supported by the Key Subjects of National Natural Science Foundation of China (Grant No. 10732090), the National Natural Science Foundation of China (Grant No. 50476004), and the 111 Project (Grant No. B08009)

nisms explained by Jimenez et al.[22] and Schoppa et al.[23−25], velocity streaks have crucial effects in the regeneration of the vortices. Thus, the weakening of velocity streaks would weaken the generation of coherent structures, which would in turn cause the reductions of turbulence intensities and drag.

The modification of streaks caused by SWO was observed by lots of researchers. The quantitative results were obtained by Cicca et al.[19] and Iuso et al.[20] with the direct measurement of streaks using PIV. They concluded: The SWO would cause the decrease of the streaks' number, the suppression of the streaks' intensities, the variation of the streaks' directions, the distortion of the streaks' configuration and the amalgamation between streaks, which gave powerful evidence for the streaks weakening mechanism.

Based on the understanding of the mechanisms of drag reduction by SWO, and the summarization of the related work, Choi et al.[15] got the quantitative relation between drag reduction and the maximum spanwise wall velocity W_m^+, and Bandyopadhyay[26] gave a deep insight into the relation, and the theoretical expression. Choi et al.[8] proposed a more comprehensive wall oscillating parameter: V_c^+, which took the depth of the influence, the amplitude of wall oscillation and the flow Reynolds number into accounts, and they found out the quadratic relation between drag reduction and V_c^+. Quadrio et al.[11,13] did further researches on the parameter V_c^+ and proposed a similar parameter: S^+. With fitting data of the related researches, they got linear relation between drag reduction and S^+.

The application of SWO technique in practice is difficult due to cost constraints, weight limitations, and so on. But some researchers still have made their efforts to gain the net energy saving. Baron et al.[4] and Quadrio et al.[11] found that, the maximum net energy saving could reach the level of 10% with proper oscillating parameters.

To sum up, there are continual researches on drag reduction through spanwise wall oscillation. So far as the author has known, there is only one numerical method for the researches in this field, that is DNS, and the flows are all incompressible. This paper presents some results about this problem by using LES of compressible turbulence, and validates the applicability of the LES. The main purposes of the paper are to analyze the influence of SWO on temperature field and heat transportation, and to get further understanding of the relation between heat and momentum transportation, as well as the mechanisms of simultaneity of drag reduction and wall heat flux reduction in some turbulence control experiment.

1 Numerical methods and validation

The three-dimensional unsteady compressible Favre-filtered Navier-Stokes equations are numerically solved. The residual subgrid stress $\tau_{ij} = \rho\left(\widetilde{u_i u_j} - \tilde{u}_i \tilde{u}_j\right)$ and sub-grid heat flux $Q_j = \overline{\rho}\left(\widetilde{u_j T} - \tilde{u}_j \tilde{T}\right)$ are modeled using dynamic SGS model:

$$\tau_{ij} - \frac{\delta_{ij}}{3}\tau_{kk} = -C2\overline{\rho}\Delta^2\left|\tilde{S}\right|\left(\tilde{S}_{ij} - \frac{\delta_{ij}}{3}\tilde{S}_{kk}\right), \tag{1}$$

$$\tau_{kk} = C_I 2\overline{\rho}\Delta^2\tilde{S}^2,$$

$$Q_j = -\frac{\overline{\rho}\nu_T}{Pr_T}\frac{\partial\tilde{T}}{\partial x_j} = -C\frac{\Delta^2\overline{\rho}\left|\tilde{S}\right|}{Pr_T}\frac{\partial\tilde{T}}{\partial x_j}, \tag{2}$$

where the coefficients C, C_I and Pr_T are calculated dynamically with the formulas:

$$C_I = \frac{1}{2\Delta^2}\frac{\langle L_{kk}\rangle}{\left\langle \hat{\overline{\rho}}\hat{\alpha}^2\hat{\tilde{S}}^2 - \hat{\overline{\rho}}\hat{\tilde{S}}^2\right\rangle},$$

$$C = \frac{\left\langle\left(L_{ij} - \frac{\delta_{ij}}{3}\right)M_{ij}\right\rangle}{\langle M_{kl}M_{kl}\rangle}, \tag{3}$$

$$Pr_T = \frac{C\langle T_k T_k\rangle}{\langle K_j T_j\rangle}.$$

The details of the symbols and modeling can be seen in the work of Martin et al.[27].

The finite volume method is employed to discretize the equations. The convectional fluxes are calculated with the fourth-order central scheme in a skew-symmetric form[28]; the diffusive fluxes are calculated with the second-order central scheme and the classic third-order three-stage Rung-Kutta method is adopted for time integral. The artificial dissipation of Swanson and Turkel[29] is incorporated to stabilize the computation. The computation and flow conditions are set as Re=3000 (based on bulk velocity and the half-high of the channel; the

corresponding friction Reynolds number: $Re_\tau \approx 180$), Mach=0.5 (based on bulk velocity and velocity of sound at wall), Prandtl=0.72; the size of the computation domain is $4\pi h \times 2h \times 4\pi h/3$ (longitude×normal×spanwise), the number of grids is 64×64×64. The mesh spacing is uniform in longitude and spanwise, and stretched in the normal direction. The boundary conditions are periodic in longitude and spanwise, and the isothermal no-slip condition is at walls.

Because of the low Mach number, the compressibility is weak, and thus we can compare the results of fixed wall channel flow with those of the incompressible DNS of Kim, Moin and Moser (KMM)[30] in the similar Reynolds number. The comparisons of mean velocity profiles and Reynolds stresses are plotted in Figure 1.

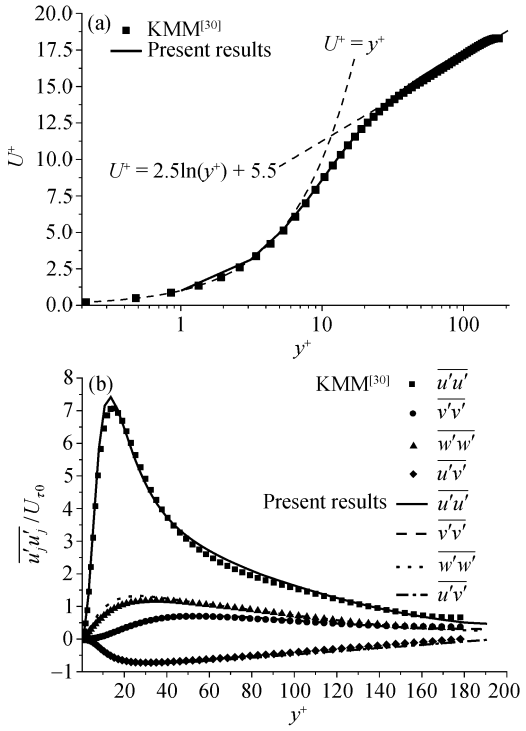

Figure 1 The comparisons of results with DNS of KMM[30]. (a) Mean velocity; (b) Reynolds stresses.

It can be seen that, the present LES results are in good agreement with those of KMM[30].

As for the temperature profile, we compare the present result with that of the LES of Lenormand et al.[31] seen in Figure 2. The present temperature profile is consistent with that of Lenormand, but a little lower. Considering that the temperature profiles of Lenormand et al.[31] are always higher than DNS results, the present result is acceptable. It can be seen from Figure 2, the temperature profile is uniform in most places of the channel; the gradient is notable only in the near wall region, which is the common characteristic of the temperature field in the channel flow that is dominated by the dissipation. Moreover, this kind of temperature field has a lot of influences on the heat transportation.

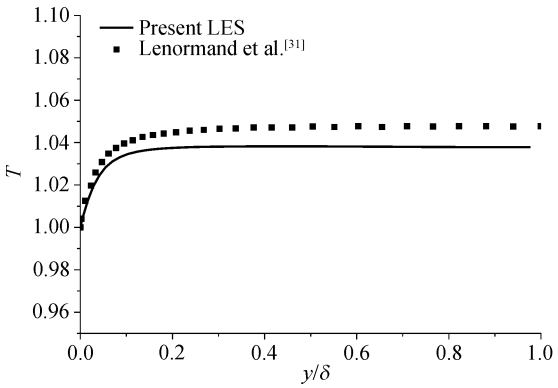

Figure 2 The mean temperature profile.

2 Descriptions and validations about SWO

Based on the former researches, the sinusoidal oscillation is used for wall movement. The spanwise wall velocity W_{wall} is expressed as

$$W_{\text{wall}} = W_{\text{m}} \sin\left(\frac{2\pi}{T_{\text{osc}}} t\right), \tag{4}$$

where W_{m} is the amplitude of the wall velocity; T_{osc} is the period of the oscillation. The wall temperature is kept constant, and the uniform longitudinal body force is imposed on to keep the mass flux a constant value which is the same as the fixed channel flow.

The period of the oscillation is chosen around $T^+_{\text{osc}} = 100$, which is optimum for drag reduction according to Jung et al.[1,2] and Baron et al.[4]. The velocity amplitude of Case C1 is that of the largest drag reduction of Jung et al.[1,2], and two larger amplitudes are also simulated for deeper understanding of the problem. Four flow cases (including the fixed wall channel) are simulated. The oscillating parameters are listed in Table 1.

Table 1 The parameters of wall oscillating

Case	T^+_{osc}	W^+_{m}	D^+_{m}
C0	unperturbed channel		
C1	104.1	6.35	204.4
C2	104.1	12.7	408.8
C3	110.4	19.05	649.2

In Table 1, Case C0 is the fixed wall channel; D_m is the peak to peak displacement of the wall; "+" stands for the variable in wall viscous scale (unless otherwise noted the friction velocity for nondimensionalizing is that of the unperturbed channel flow C0).

With the oscillating of the wall, the drags are largely reduced. The evolutions of ratios of wall shear stresses τ_w to the averaged value in the unperturbed channel τ_{w0} of each case are plotted in Figure 3.

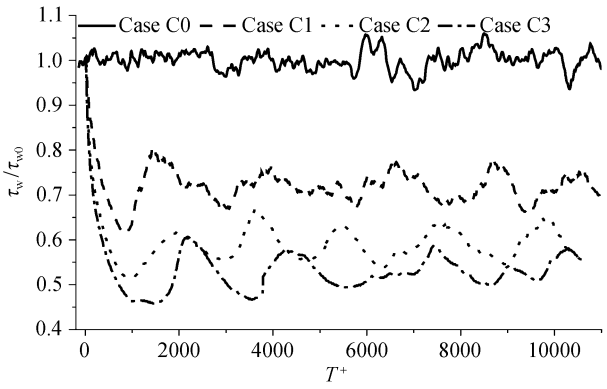

Figure 3 The evolutions of the drag ratio.

At about 8 periods after the oscillation started ($T^+ \approx 8T^+_{osc}$), the wall shear stress reaches the minimum value, which is consistent with the result of Jung et al.[1,2]. Then, the flow reaches the state of statistical steady low drag, and with the increase of the oscillating amplitude, the drag reduction increases.

The comparisons of the drag reduction data with other researches are carried out to validate the reliability of the LES for simulating such problems. Three different methods of describing the oscillation are used for comparisons. The drag reduction ratio is defined as

$$\mathrm{DR} = \frac{\tau_w - \tau_{w0}}{\tau_{w0}} \times 100\%. \quad (5)$$

The DRs of the present simulated cases are listed in Table 2.

Table 2 The drag reduction ratio (DR)

Case	DR (%)
C1	28
C2	40
C3	46

Three methods of describing oscillation and drag reduction relations which were proposed by Choi et al.[8,15] and Riccoa et al.[13] respectively are employed for the validation. The comparisons can be seen in Figures 4—6.

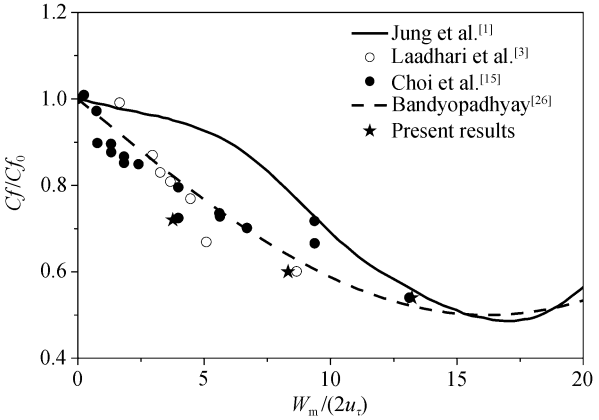

Figure 4 Drag reduction as a function of spanwise wall velocity: $W_m/(2u_\tau)$[15].

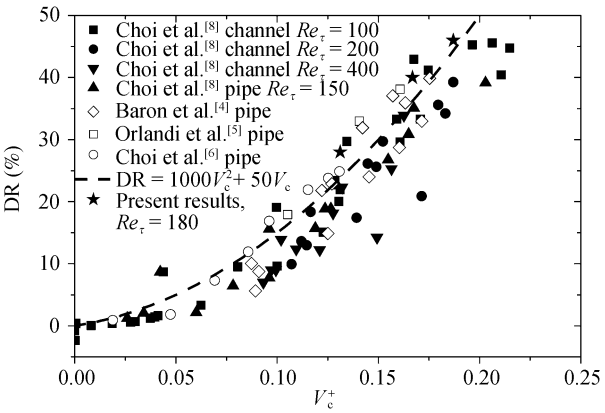

Figure 5 Drag reduction as a function of V_c^+. V_c^+ is the parameter describing wall oscillation, which considers the strength and the influence range of the Stokes layer caused by wall oscillation. The details of the definition can be seen in ref. [8].

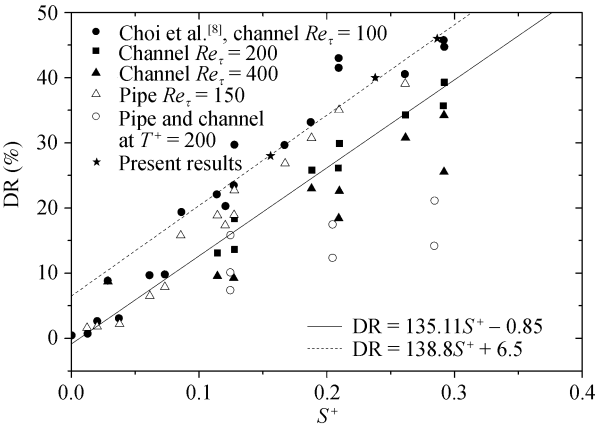

Figure 6 Drag reduction as a function of S^+. S^+ has the similar meaning with V_c^+ in Figure 5. The details of the definition can be seen in ref. [13].

It can be seen that, with different ways of describing oscillation, the relations of drag reduction to these parameters of present study are in good agreement with the

published results (DNSs and experiments). Although there are still some divarications, the situation is acceptable considering the similar divarications among the published results. Based on these analyses, the reliability of present LES for such problems and the results are sufficiently validated.

3 Results and analyses

Based on the published results of the SWO in incompressible turbulence, the compressible turbulence is analyzed. The modifications of temperature field and heat transportation are highly emphasized, as well as the relations with velocity field and momentum transportation.

3.1 Mean statistics and analyses

The distributions of mean velocities of all the cases are presented in Figure 7.

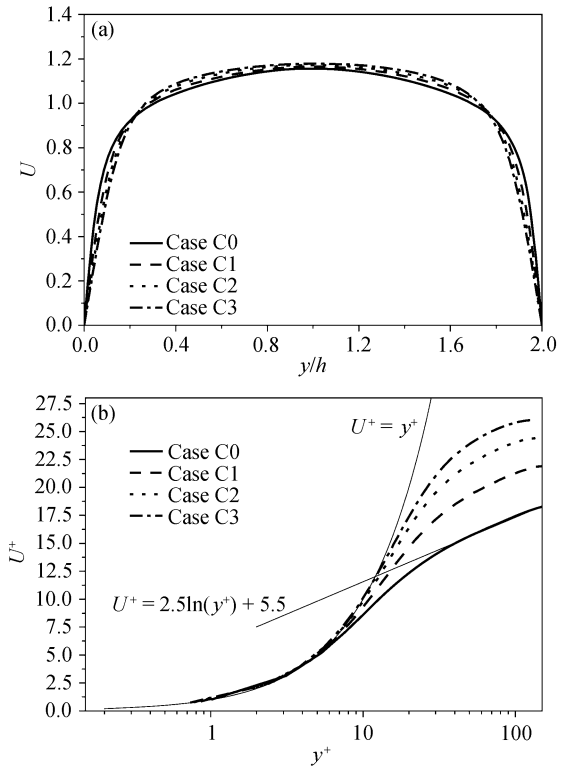

Figure 7 The mean velocity profile. (a) The channel scale; (b) the wall scale (local friction velocity is used for scaling).

According to Figure 7(a), the velocity of the near wall layer is reduced due to the oscillation, which will cause the reduction of velocity gradient and wall stress. And with the increase of the drag reduction ratio, the reduction of the near wall layer velocity will also increase. While at the channel central region, because of the restriction of mass conservation, the velocity is higher than that of the unperturbed cases. With the comparisons of U^+ (nondimensionalized using local friction velocity) in Figure 7(b), the SWO will cause the thickening of linear region and the rise of the log layer and the tendency is stronger with the increase of the drag reduction. This kind of modification of velocity is observed in other drag reduction turbulence (such as surfactant solution or riblets) when the turbulence activity is suppressed.

The influence of SWO on wall heat flux is different from the drag (streamwise). The near wall spanwise Stokes layer induced by wall oscillation produces dissipation which has a strong heat effect on wall. The phase of Stokes layer and dissipation changes with wall oscillation, and it will cause the variation of wall heat flux with oscillation. The period of variation of wall heat flux and dissipation is about one half of the period of the wall oscillation. The variation of a period of the heat flux with time is plotted in Figure 8.

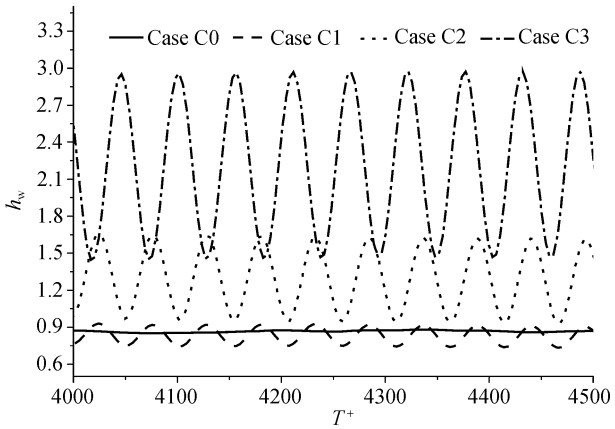

Figure 8 The evolution of wall heat flux.

It can be seen that with the increase of oscillating amplitude, the average wall heat flux and the amplitude of its variation also increase. This is due to the strength and variation amplitude of Stokes layer increase with the increase of the oscillating amplitude, and accordingly the strength and variation amplitude of dissipation also increase. Basically the Stokes layer caused by SWO is a laminar flow, and that is the reason for the regular variation of wall heat flux. Basically, it is sinusoidal.

The effects of SWO on wall heat flux can be divided into three aspects: 1) The increase effect by adding dissipation that is caused by induced spanwise Stokes layer;

2) the decrease effect by reducing dissipation that is caused by the reduction of streamwise velocity gradients with the suppression of turbulent intensity; 3) the decrease effect by the suppression of turbulent heat transportation from the channel central to the wall.

The above three effects are in different proportions with different oscillating parameters, and the wall heat flux could increase or decrease. The time average wall heat fluxes ratio h_w/h_{w0} of all the cases are listed in Table 3.

Table 3 The ratio of wall heat flux to that in the unperturbed channel

Case	h_w/h_{w0}
C1	0.95
C2	1.5
C3	2.5

With the proper oscillating parameter (such as: Case C1), the average wall heat flux can be reduced. This gives the theoretical possibility to employ SWO in the control of surface temperature, thermal load and infrared radiation.

The average temperature profiles for all the cases are plotted in Figure 9.

It can be seen, in the cases of large amplitude oscillation (C2 and C3), the mean temperature is higher than the Case C0 in the whole channel because of the high dissipation. In the case of small amplitude oscillation (C1), the mean temperature is still higher than Case C0 in the most place of the channel, but in the near wall region, the temperature is lower. This is because of the suppression of heat transportation between central region and near wall region. Even the total internal energy is increased; the suppression of heat transportation can reduce the temperature in the near wall region, and cause the reduction of average wall heat flux.

The Cases C0 and C1 are further studied for turbulence fluctuations statistic and turbulence structures. The results of C2 and C3 are similar to that of C1with only quantity differences.

The distributions of turbulent intensities $\overline{u_i'u_i'}/U_{\tau 0}^2$ are plotted in Figure 10.

The turbulent intensities are largely suppressed by SWO C1; and the position of peak values of $\overline{u_i'u_i'}/U_{\tau 0}^2$ moves towards the channel center. These phenomena have been observed by other researchers. It should be noted that the intensity of spanwise velocity fluctuation $\overline{w'w'}$ has very large values in the near wall region. That

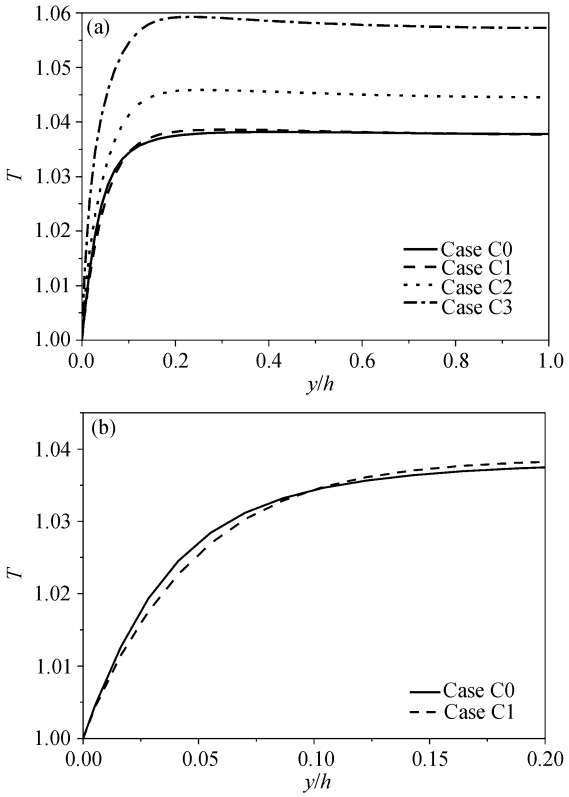

Figure 9 The mean temperature profiles. (a) Across the channel; (b) zoom for Case C0 and C1.

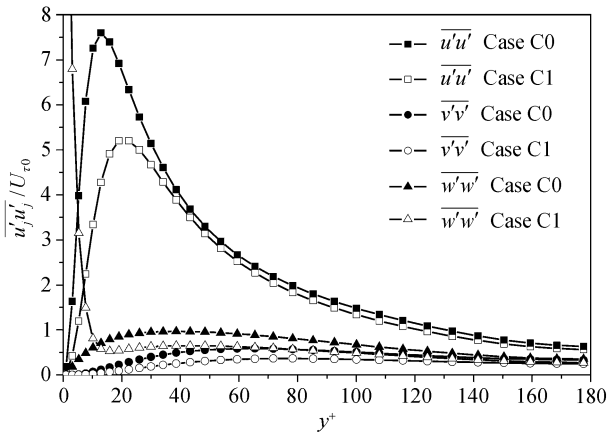

Figure 10 Turbulent intensity.

is caused by the statistical method we adopt here, which takes account of the Stokes velocity as spanwise fluctuation. This part of the fluctuation is not attributed to the turbulence, and the influence range of the Stokes layer is about $y^+<15$; beyond that range the spanwise fluctuation is normal and lower than Case C0.

The temperature fluctuation intensity is also reduced by SWO, as plotted in Figure 11, where the friction temperature is the one in the unperturbed channel flow,

which is defined as $T_{\tau 0}=\dfrac{k}{\rho C_P U\tau}\dfrac{\partial \overline{T}}{\partial y}\bigg|_{\mathrm{w}}$.

Compared with velocity fluctuations, the temperature fluctuation is much smaller beyond the region of $y^+<40$. The reason is as follows: The mean temperature profile is quite uniform in the central region of the channel (Figures 2 and 9), and the turbulence vortex movement cannot generate intense temperature transportation and fluctuation on the uniform mean temperature distribution; while, in the near wall region, the temperature gradient is large, and so does the temperature fluctuation.

The temperature fluctuation intensity is dramatically reduced by the SWO, which is consistent with the velocity fluctuations.

3.2 Statistics and analysis about turbulence structure

Based on former researches, the SWO can effectively suppress the generation of turbulence coherent structures. The turbulence coherent structures can be denoted by the isosurface of λ_2, whose definition and physical meaning can be seen in ref. [32]. The distributions of coherent structures in the turbulent channel flow at different time under the wall oscillation (C1) are plotted in Figure 12.

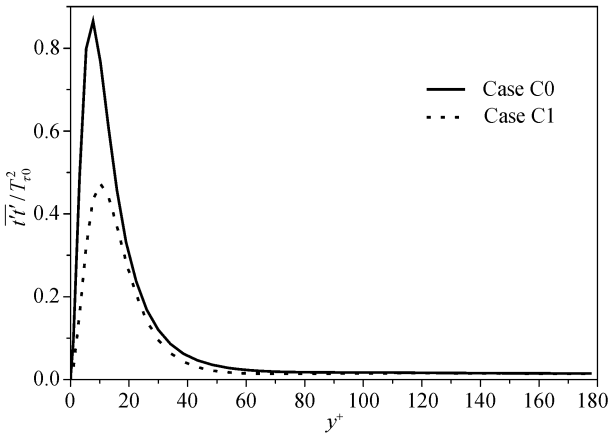

Figure 11 Turbulence temperature fluctuation intensity.

The generation of coherent structures is effectively suppressed, which can be seen from the decrease of the density of the coherent structures. At the time of the lowest wall stress (T^+=825, Figure 12(c)), the coherent structures can hardly be found, and the flow is nearly laminar.

The spanwise wall movement also has strong influences on the near wall streaks. The streaks (both velocity streaks and temperature streaks) at $y^+\approx 10$ are plotted in Figure 13.

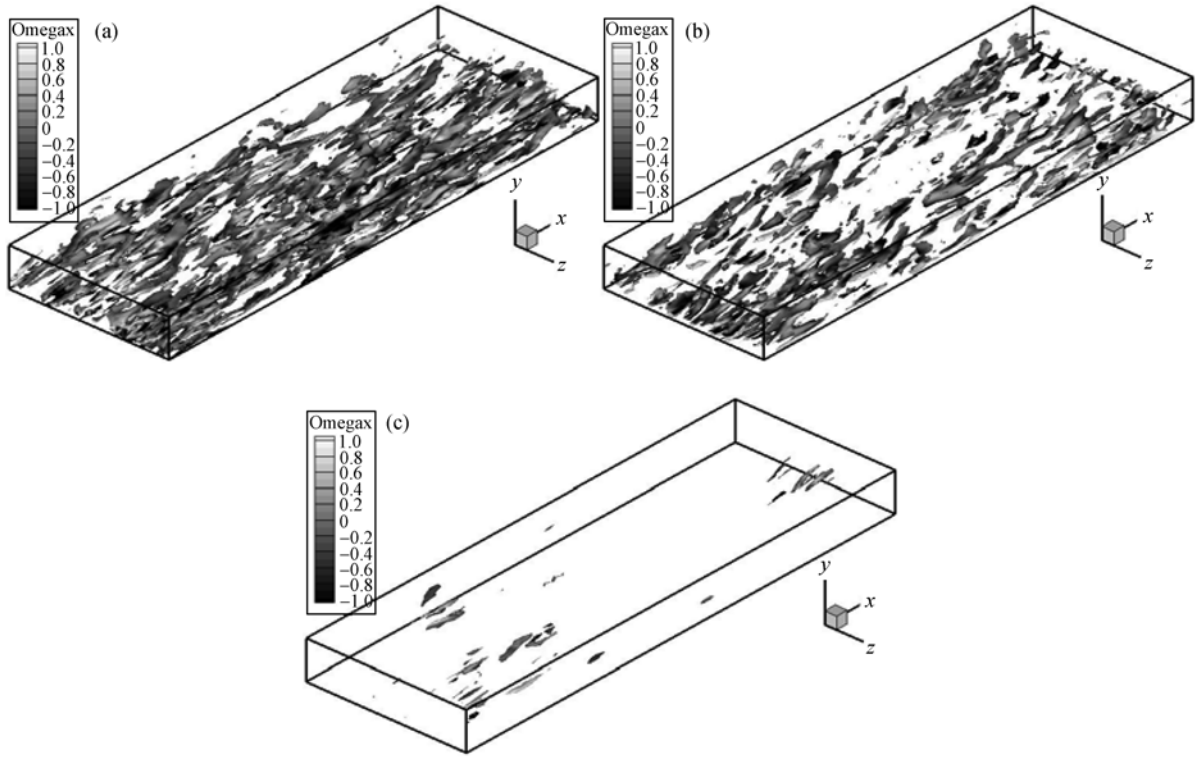

Figure 12 The evolution of the coherent structure of Case C1 (isosurface of λ_2 and colored by contours of streamwise vorticity). (a) T^+=0; (b) T^+=400; (c) T^+=825.

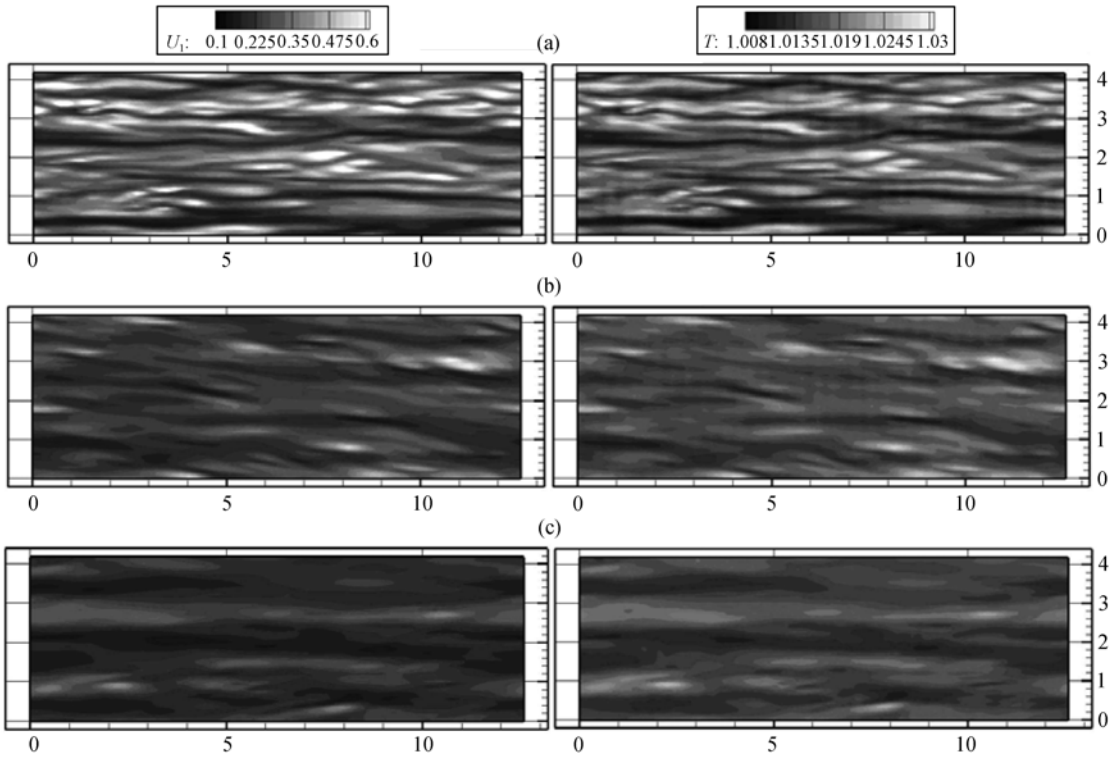

Figure 13 The streaks at $y^+\approx10$ of Case C1 (left: velocity streaks; right: temperature streaks). (a) $T^+=0$; (b) $T^+=400$; (c) $T^+=825$.

It can be seen that, under the influences of SWO, the direction of streaks keeps varying; the width of streaks increases and the strength of the steaks is weakened. These characteristics of the modification are consistent with the reported results of Choi et al.[15], Cicca et al.[19] and Iuso et al.[20].

The temperature streaks are also analyzed in comparison with the velocity streaks. The strong consistency and the corresponding relation of velocity streaks and temperature streaks in natural wall turbulence are widely observed and reported (Iritani et al.[33], Kong et al.[34]). From the present work, the velocity streaks and temperature streaks still keep in good consistency and corresponding relation under the influences of SWO. The SWO changes both velocity streaks and temperature streaks dramatically, but it can barely change the relationship between them. This demonstrates that the generation mechanisms of velocity streaks and temperatures streaks are the same.

The fluctuations of coherent structures (mostly quasi-longitude vortexes in the boundary layer flow) are the main reason of the higher transportation of turbulent flow compared with the laminar flow. Thus, the modification of coherent structures will have strong effects on the transportation of turbulent boundary layer. The statistics of Reynolds shear stress $\overline{u'v'}$ and normal turbulent heat flux $\overline{t'v'}$ which are the main contributors of momentum and heat transportation respectively are analyzed.

The distribution of $\overline{u'v'}$ is plotted in Figure 14. It can be seen that, the SWO reduces the absolute value of $\overline{u'v'}$ in the whole channel effectively, and the peak position moves slightly towards the center. It demonstrates that the transportation of momentum is remarkably suppressed, which is the main reason for the reduction of

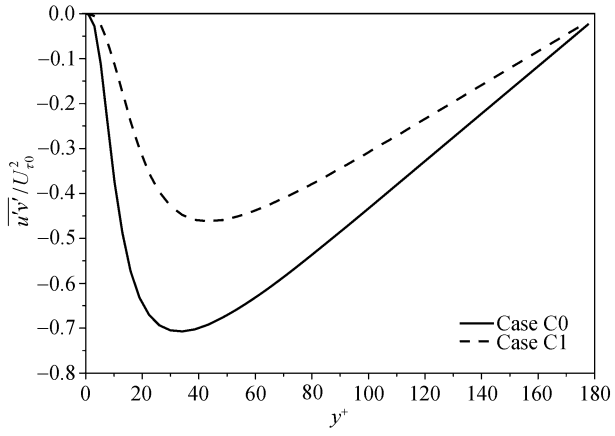

Figure 14 Distribution of Reynolds shear stress: $\overline{u'v'}$.

drag.

The correlation of u' and v': $R(u',v')$ (defined as $R(u',v')=\overline{u'v'}/(\sqrt{\overline{u'^2}}\sqrt{\overline{v'^2}})$)is calculated here to study the embedded reason for the reduction of $\overline{u'v'}$, as plotted in Figure 15.

It is noticeable in Figure 15 that, for unperturbed channel flow, the $R(u',v')$ has a local peak at $y^+\approx12$. It is also reported by Kim, Moin and Moser[30], and they said "$y^+\approx12$… which is also the location of the maximum production and the maximum streamwise velocity fluctuation…where it was attributed to a certain organized motion in the wall region." It is found that, the local peak disappears in the channel with SWO. The distribution in the whole channel is quite smooth comparatively, and the most significant difference of the $R(u',v')$ between Cases C0 and C1 appears at $y^+\approx12$. It demonstrates that the certain organized motion in the wall region is modified by SWO; it is weakened or annihilated. In addition, the $R(u',v')$ for Case C1 is smaller than that in Case C0 across the entire channel, which demonstrates the organized turbulent motion across the entire channel is weakened.

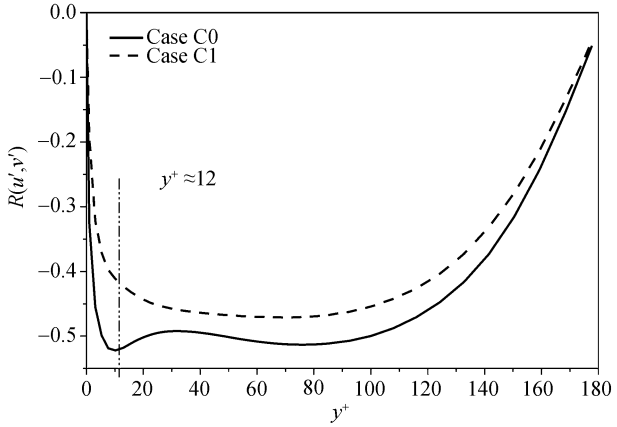

Figure 15 Distribution of $R(u',v')$.

To study the heat transportation, the distribution of normal turbulent heat flux $\overline{t'v'}$ is plotted in Figure 16.

It can be seen that, in the near wall region, $\overline{t'v'}$ is remarkably reduced and the peak position moves towards the central, which is consistent with $\overline{u'v'}$. It shows that the SWO reduces the transportation of both momentum and heat simultaneously.

The correlation coefficient of t' and v' is also calculated, as plotted in Figure 17.

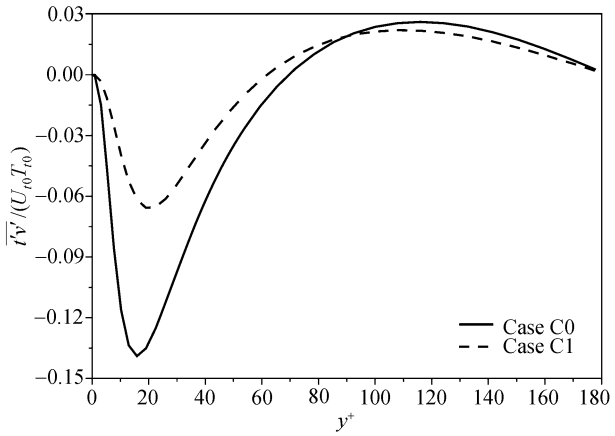

Figure 16 Distribution of normal turbulent heat flux: $\overline{t'v'}$.

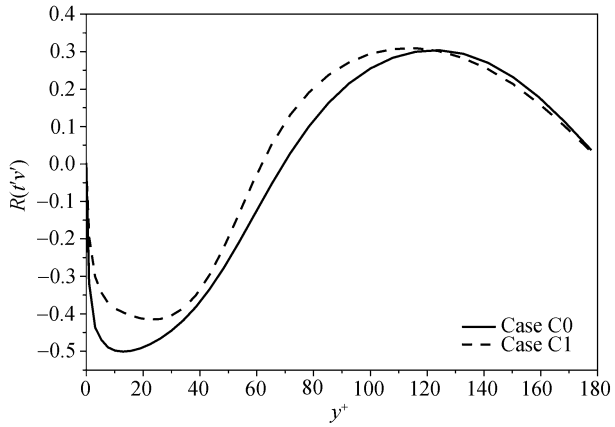

Figure 17 Distribution of $R(t',v')$.

Comparing the $R(u',v')$ with $R(t',v')$, we find that, no matter whether there is an oscillation, the distribution of $R(u',v')$ keeps a high value in the region of $y^+<100$, while $R(t',v')$ falls-off remarkably where $y^+>40$. This characteristic of the distribution of $R(t',v')$ is consistent with the distributions of mean temperature (Figure 9) and temperature fluctuation (Figure 11). The reason is that, at the region of $y^+>40$, the mean temperature is quite uniform; the movement of turbulent vortex can hardly cause the heat transportation due to the lack of the temperature gradient. Thus, the correlation coefficient that stands for turbulent structures is very small.

But in the near wall region, there are still some common characteristics for $R(u',v')$ and $R(t',v')$. In the unperturbed channel flows, they both have peak values at $y^+\approx12$, and this demonstrates that the organized turbulent motion has crucial effects on the transportations of both moment and heat. Meanwhile, when the SWO is imposed, $y^+\approx12$ is the position where the difference of the coefficients is the most for both $R(u',v')$ and $R(t',v')$, in

the near wall region. This demonstrates that the modification of turbulent structures by SWO has similar suppressing effects on the transportations of both momentum and heat.

4 Conclusions

The channel turbulent flow with spanwise wall oscillation is simulated using LES, to study the influences of SWO on temperature field and heat transportation and the capability of the LES for such controlled turbulent flow. Some results are reached:

(i) Three flow cases with different oscillation parameters are simulated. Using different methods of describing oscillation, the drag reduction data we get are consistent with the data of other researchers who used DNS or experiment. And the capability LES and reliability of results for such controlled turbulent flow are sufficiently validated.

(ii) The SWO can effectively suppress the generation of coherent structures in the turbulent boundary layer, and causes the reductions of the transportations of moment and heat, the decreases of the fluctuation intensities of velocity and temperature, as well as the reduction of wall shear stress.

(iii) The velocity streaks and temperature streaks keep good consistency and the corresponding relations all the time, even they are both dramatically changed by SWO. This demonstrates that the SWO has the same effects on both velocity streaks and temperature streaks. The mechanism is the same dominant effects of coherent structures on moment transportation and heat transportation in turbulent flows.

(iv) Even if the Stokes layer caused by SWO will induce added dissipation, the average wall heat flux could be reduced with properly choosing of oscillating parameter (e.g. Case C1), because of the suppression of heat transfer and dissipation caused by streamwise velocity.

The authors would like to thank Dr. Ye Jian for offering the original LES codes, and Prof. He Guowei, Prof. Xu Chunxiao and Ms. Fang Juan for their valuable suggestions and generous help.

1 Jung W J, Mangiavacchi N, Akhavan R. Suppression of turbulence in wall-bounded flows by high-frequency spanwise oscillations. Phys Fluids A, 1992, 4(8): 1605－1607
2 Akhavan R, Jung W J, Mangiavacchi N. Control of wall turbulence by high frequency spanwise oscillation. In: Shear Flow Conference. Orlando: AIAA, 1993. AIAA-93-3282
3 Laadhari F, Skandaji L, Morel R. Turbulence reduction in a boundary layer by a local spanwise oscillating surface. Phys Fluids, 1994, 6(10): 3218－3220
4 Baron A, Quadrio M. Turbulent drag reduction by spanwise wall oscillations. Appli Sci Res, 1996, 55(4): 311－326
5 Orlandi P, Fatica M. Direct simulations of turbulent flow in a pipe rotating about its axis. J Fluid Mech, 1997, 343: 43—72
6 Dhanak M R, Si C. On reduction of turbulent wall friction through spanwise wall oscillations. J Fluid Mech, 1999, 383: 175－195
7 Quadrio M, Sibilla S. Numerical simulation of turbulent flow in a pipe oscillating around its axis. J Fluid Mech, 2000, 424: 217－241
8 Choi J I, Xu C-X, Sung H J. Drag reduction by spanwise wall oscillation in wall-bounded turbulent flows. AIAA J, 2002, 40(5): 842－850
9 Huang X W, Xu C X, Cui G X, et al. The influence of spanwise wall oscillation on the transportation of Reynolds stress. In: Proceedings of 2003' Fluid Mechanics Youth Workshop, 2003. 206－211
10 Huang W X, Xu C X, Cui G X, et al. Mechanism of drag reduction by spanwise wall oscillation in turbulent channel flow. Acta Mech Sin, 2004, 36(1): 24－30
11 Quadrio M, Ricco P. Critical assessment of turbulent drag reduction through spanwise wall oscillations. J Fluid Mech, 2004, 521: 251－271
12 Zhou D, Ball K S. The Mechanism of turbulent drag reduction by spanwise wall oscillation. In: 42nd AIAA/ASME/SAE/ASEE Joint Propulsion Conference & Exhibit. Sacramento, California, 2006. 1－14
13 Riccoa P, Quadrio M. Wall-oscillation conditions for drag reduction in turbulent channel flow. Int J Heat Fluid Flow, 2008, 29(4): 891－902
14 Trujillo S M, Bogard D G, Ball K S. Turbulent boundary layer drag reduction using an oscillating wall. AIAA Paper, 1997, AIAA-1997-1870
15 Choi K-S, DeBisschop J R, Clayton B R. Turbulent boundary-layer control by means of spanwise-wall oscillation. AIAA J, 1998, 36(7): 1157－1163
16 Choi K-S, Graham M. Drag reduction of turbulent pipe flows by circular-wall oscillation. Phys Fluid, 1998, 10(1): 1－9
17 Choi K-S, Clayton B R. The mechanism of turbulent drag reduction with wall oscillation. Int J Heat Fluid Flow, 2001, 22: 1－9
18 Choi K-S. Near-wall structure of turbulent boundary layer with spanwise-wall oscillation. Phys Fluid, 2002, 14(7): 2530－2542
19 Cicca G M D, Iuso G, Spazzini P G, et al. Particle image velocimetry investigation of a turbulent boundary layer manipulated by spanwise wall oscillations. J Fluid Mech, 2002, 467: 41－56
20 Iuso G, Cicca G M D, Onoratob M, et al. Velocity streak structure modifications induced by flow manipulation. Phys Fluid, 2003, 15(9): 2602－2612
21 Ricco P, Wu S. On the effects of lateral wall oscillations on a turbulent

boundary layer. Exp Thermal Fluid Sci, 2004, 29(1): 41－52
22 Jimenez J, Pinelli A. Wall Turbulence: How it works and how to damp it. In: The 4th AIAA Shear Flow Control Conference. Snowmass, 1997, AIAA-97-2112
23 Schoppa W, Hussain F. Formation of near-wall streamwise vortices by streak instability. Technical Report 98-3000, In: AIAA, 29th AIAA Fluid Dynamics Conference, Albuquerque, NM, USA, 1998
24 Schoppa W, Hussain F. Coherent structure dynamics in near-wall turbulence. Fluid Dynamics Res, 2000, 26: 118－139
25 Schoppa W, Hussain F. Coherent structure generation in near-wall turbulence. J Fluid Mech, 2002, 453: 57－108
26 Bandyopadhyay P R. Stokes mechanism of drag reduction. J Appl Mech, 2006, 73: 483－489
27 Martin M P, Piomelli U, Candler G V. Subgrid-scale models for compressible large-eddy simulation. Theorel Comput Fluid Dynamics, 2000, 13: 161－376
28 Ducros F, Laporte F, Souléres T, et al. High-order fluxes for conservative skew-symmetric-like scheme in structured meches: Application to compressible flows. J Compt Phys, 2000, 116: 114－139
29 Swanson R C, Turkel E. On central-difference and upwind schemes, J Compt Phys, 1992, 101: 292－306
30 Kim J, Moin P, Moser R. Turbulence statistics in fully developed channel flow at low Reynolds number. J Fluid Mech, 1987, 177: 133－166
31 Lenormand E, Sagaut P, Pbuoc L T. Large eddy simulation of subsonic and supersonic channel flow at moderate Reynolds number. Int J Numer Methods Fluids, 2002, 32: 269－406
32 Jeong J, Hussain F. On the identification of a vortex. J Fluid Mech, 1994, 285: 69－94
33 Iritani Y, Kasagi N, Hirata M. Heat transfer mechanism and associated turbulence structure in the near-wall region of a turbulent Boundary Layer. In: Turbulent Shear Flows 4: Selected papers from the 4th International Symposium on Turbulent Shear, University of Karlsruhe. 1983. 223－234
34 Kong H, Choi H, Lee J K. Direct numerical simulation of turbulent thermal boundary layers. Phys Fluids, 2000, 12(10): 2555－2568